A Supplementary material for LHCb-PAPER-2019-020

A.1 Details on the energy variation fit

The four ratios of efficiency corrected $B_s^0 \to J/\psi\,\phi$ and $B^+ \to J/\psi\,K^+$ yields are fitted with a linear function: $a + k_s \cdot \sqrt{s}$. The ratios are correlated due to the common tracking efficiency systematic uncertainties and due to the common (0.8%) systematic uncertainty assigned to the fitted $B_s^0 \to J/\psi\,\phi$ yield in order to account for additional resonant and nonresonant contributions. The following covariance matrix is used to account for the correlations in the χ^2 fit:

$$\begin{pmatrix} 5.737 & 3.351 & 3.948 & 3.790 \\ 3.351 & 5.471 & 4.049 & 3.886 \\ 3.948 & 4.049 & 9.219 & 4.579 \\ 3.790 & 3.886 & 4.579 & 5.595 \end{pmatrix} \times 10^{-6}.$$

A.2 Fitted B-meson mass distributions

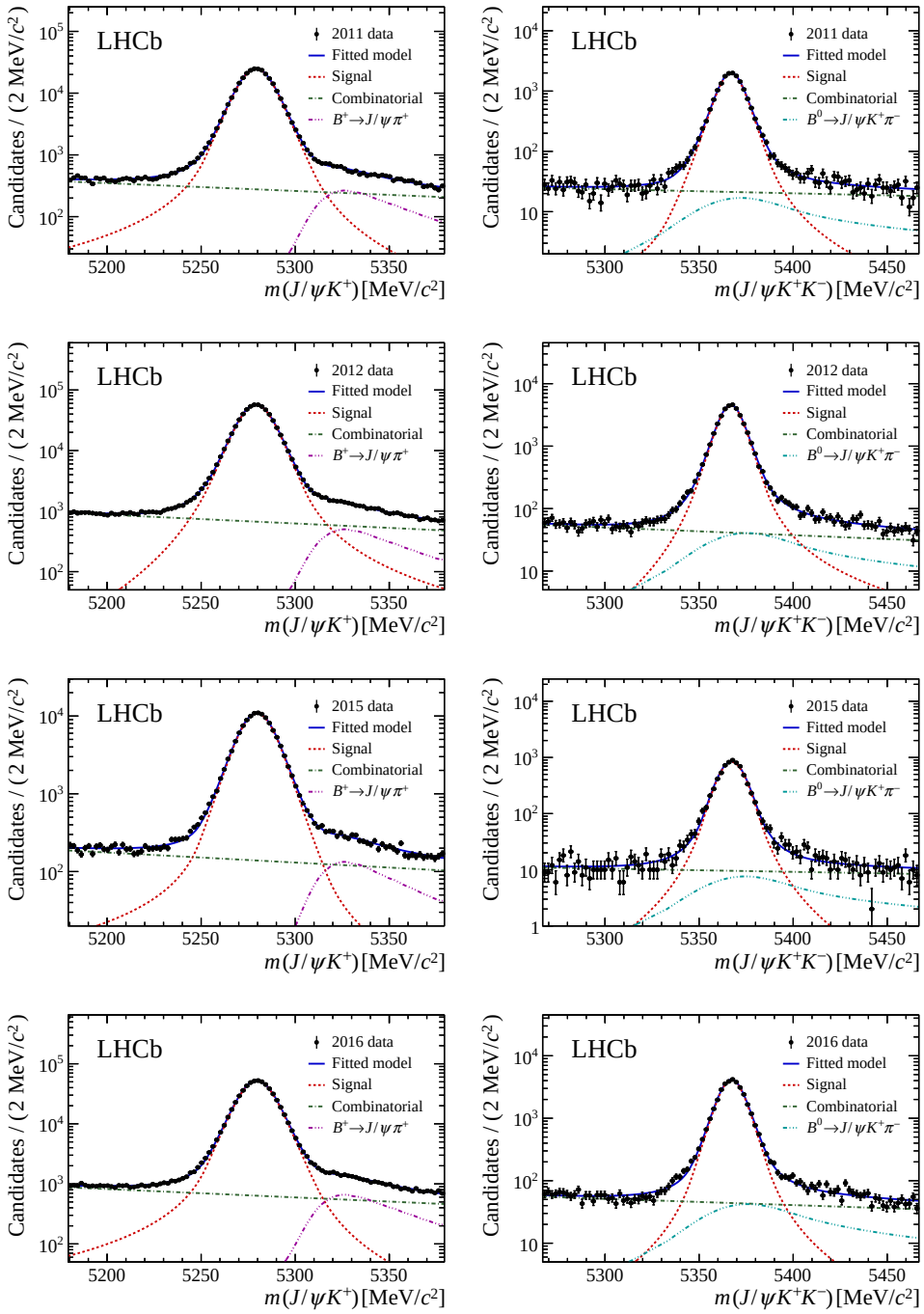

Figure 4: The B-meson mass distributions of (left column) $B^+ \to J/\psi K^+$ and (right column) $B_s^0 \to J/\psi\phi$ candidates in LHCb data collected in 2011, 2012, 2015, and 2016, shown from top to bottom in that order. The result of the fit is drawn with a blue solid line. The model components are denoted with the dashed lines: signal in red, combinatorial background in green, misidentified $B^+ \to J/\psi\pi^+$ in magenta and the misidentified inclusive $B_s^0 \to J/\psi\phi$ contribution in light blue.

A.3 Plotted ratios in bins of p^{B} and y^{B}

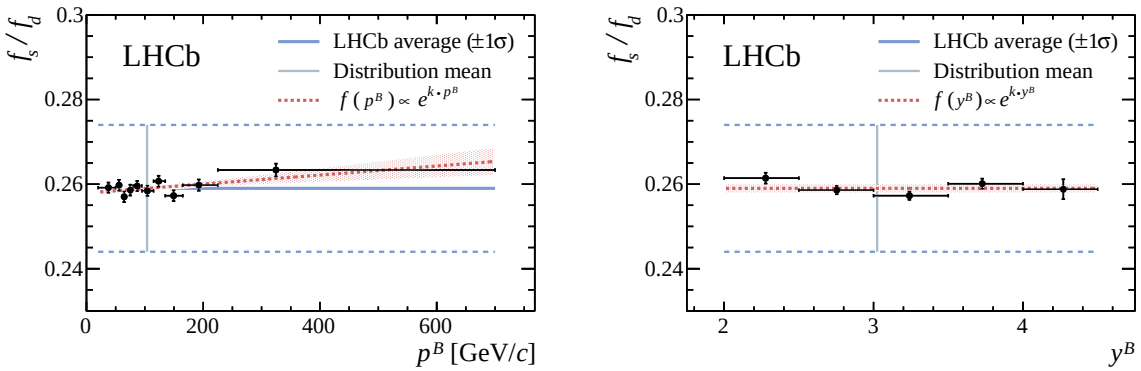

Figure 5: Efficiency-corrected $B_s^0 \to \mathrm{J}/\psi\,\phi$ and $B^+ \to \mathrm{J}/\psi\,K^+$ yield ratios ($\mathcal{R}$) in bins of B-meson momentum p^{B} (left) and rapidity y^{B} (right). The ratios are scaled to match the measured f_s/f_d value (horizontal blue lines, the $\pm1\sigma$ interval is indicated by the dashed blue lines) at the positions indicated by the vertical gray lines. The red dashed line denotes the result of the exponential fit used to estimate the statistical significance of the variation (see text), and the red band denotes the 68% confidence region.

A.4 Numerical and plotted ratios in bins of ${p_{\mathrm{T}}}^{\mathrm{B}}$ for $p_{\mathrm{L}}^{\mathrm{B}}$ subregions

Table 1: The efficiency-corrected yield ratio ($\mathcal{R}$) in bins of B-meson transverse momentum in (a) low, (b) medium, and (c) high B-meson longitudinal-momentum regions. Uncertainties include both statistical and systematic sources.

a) $0 \le p_{\mathrm{L}}^{\mathrm{B}} < 75\,\mathrm{GeV}/c$

Range [GeV/c]	$\mathcal{R}$
$0.5 < {p_{\mathrm{T}}}^{\mathrm{B}} < 4$	0.124 ± 0.002
$4 < {p_{\mathrm{T}}}^{\mathrm{B}} < 6$	0.127 ± 0.003
$6 < {p_{\mathrm{T}}}^{\mathrm{B}} < 8$	0.129 ± 0.003
$8 < {p_{\mathrm{T}}}^{\mathrm{B}} < 11$	0.125 ± 0.004
$11 < {p_{\mathrm{T}}}^{\mathrm{B}} < 40$	0.119 ± 0.006

b) $75 \le p_{\mathrm{L}}^{\mathrm{B}} < 125\,\mathrm{GeV}/c$

Range [GeV/c]	$\mathcal{R}$
$0.5 < {p_{\mathrm{T}}}^{\mathrm{B}} < 4$	0.128 ± 0.003
$4 < {p_{\mathrm{T}}}^{\mathrm{B}} < 6$	0.132 ± 0.003
$6 < {p_{\mathrm{T}}}^{\mathrm{B}} < 8$	0.128 ± 0.003
$8 < {p_{\mathrm{T}}}^{\mathrm{B}} < 11$	0.129 ± 0.003
$11 < {p_{\mathrm{T}}}^{\mathrm{B}} < 40$	0.119 ± 0.003

c) $125 \le p_{\mathrm{L}}^{\mathrm{B}} < 700\,\mathrm{GeV}/c$

Range [GeV/c]	$\mathcal{R}$
$0.5 < {p_{\mathrm{T}}}^{\mathrm{B}} < 4$	0.131 ± 0.004
$4 < {p_{\mathrm{T}}}^{\mathrm{B}} < 6$	0.128 ± 0.004
$6 < {p_{\mathrm{T}}}^{\mathrm{B}} < 8$	0.127 ± 0.003
$8 < {p_{\mathrm{T}}}^{\mathrm{B}} < 11$	0.123 ± 0.003
$11 < {p_{\mathrm{T}}}^{\mathrm{B}} < 40$	0.121 ± 0.002

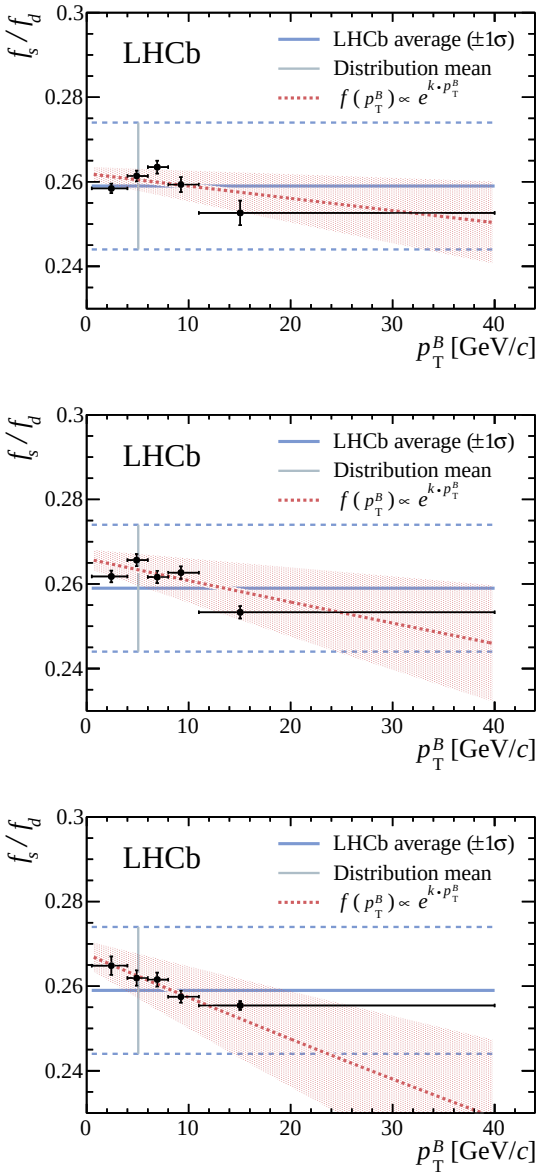

Figure 6: Efficiency-corrected $B_s^0 \to J/\psi\,\phi$ and $B^+ \to J/\psi\,K^+$ yield ratios ($\mathcal{R}$) in bins of B-meson transverse momentum $p_T{}^B$, shown for the B-meson longitudinal-momentum ranges: (top) low range ([0,75) GeV/c), (middle) medium range ([75,125) GeV/c), and (bottom) high range ([125,700] GeV/c). The ratios are scaled to match the measured f_s/f_d value (horizontal blue lines, the $\pm1\sigma$ interval is indicated by the dashed blue lines) at the positions indicated by the vertical gray lines. The red dashed line denotes the result of the exponential fit used to estimate the variation (see text), and the red band denotes the 68% confidence region.

A.5 Numerical ratios in bins of p^{B}, $p_{\mathrm{L}}^{\mathrm{B}}$, ${p_{\mathrm{T}}}^{\mathrm{B}}$, η^{B}, and y^{B}

Table 2: The measured efficiency-corrected yield ratio ($\mathcal{R}$) in bins of the kinematic variables. Uncertainties include both statistical and systematic sources.

(a) Results as a function of the total B-meson momentum.

Range [GeV/c]	$\mathcal{R}$
$20 < p^{\mathrm{B}} < 50$	0.127 ± 0.002
$50 < p^{\mathrm{B}} < 60$	0.127 ± 0.003
$60 < p^{\mathrm{B}} < 70$	0.125 ± 0.003
$70 < p^{\mathrm{B}} < 80$	0.126 ± 0.003
$80 < p^{\mathrm{B}} < 95$	0.127 ± 0.002
$95 < p^{\mathrm{B}} < 110$	0.126 ± 0.002
$110 < p^{\mathrm{B}} < 135$	0.128 ± 0.003
$135 < p^{\mathrm{B}} < 165$	0.125 ± 0.003
$165 < p^{\mathrm{B}} < 225$	0.127 ± 0.003
$225 < p^{\mathrm{B}} < 700$	0.131 ± 0.003

(b) Results as a function of the B-meson longitudinal momentum.

Range [GeV/c]	$\mathcal{R}$
$20 < p_{\mathrm{L}}^{\mathrm{B}} < 50$	0.126 ± 0.002
$50 < p_{\mathrm{L}}^{\mathrm{B}} < 60$	0.127 ± 0.003
$60 < p_{\mathrm{L}}^{\mathrm{B}} < 70$	0.125 ± 0.003
$70 < p_{\mathrm{L}}^{\mathrm{B}} < 80$	0.127 ± 0.003
$80 < p_{\mathrm{L}}^{\mathrm{B}} < 95$	0.127 ± 0.002
$95 < p_{\mathrm{L}}^{\mathrm{B}} < 110$	0.127 ± 0.003
$110 < p_{\mathrm{L}}^{\mathrm{B}} < 135$	0.127 ± 0.002
$135 < p_{\mathrm{L}}^{\mathrm{B}} < 165$	0.125 ± 0.003
$165 < p_{\mathrm{L}}^{\mathrm{B}} < 225$	0.127 ± 0.003
$225 < p_{\mathrm{L}}^{\mathrm{B}} < 700$	0.130 ± 0.003

(c) Results as a function of the B-meson transverse momentum.

Range [GeV/c]	$\mathcal{R}$
$0.5 < {p_{\mathrm{T}}}^{\mathrm{B}} < 2$	0.125 ± 0.003
$2 < {p_{\mathrm{T}}}^{\mathrm{B}} < 3$	0.127 ± 0.003
$3 < {p_{\mathrm{T}}}^{\mathrm{B}} < 4$	0.125 ± 0.003
$4 < {p_{\mathrm{T}}}^{\mathrm{B}} < 5$	0.128 ± 0.003
$5 < {p_{\mathrm{T}}}^{\mathrm{B}} < 6$	0.128 ± 0.003
$6 < {p_{\mathrm{T}}}^{\mathrm{B}} < 7$	0.127 ± 0.003
$7 < {p_{\mathrm{T}}}^{\mathrm{B}} < 8$	0.127 ± 0.003
$8 < {p_{\mathrm{T}}}^{\mathrm{B}} < 9$	0.126 ± 0.003
$9 < {p_{\mathrm{T}}}^{\mathrm{B}} < 10$	0.125 ± 0.003
$10 < {p_{\mathrm{T}}}^{\mathrm{B}} < 11.5$	0.125 ± 0.003
$11.5 < {p_{\mathrm{T}}}^{\mathrm{B}} < 14$	0.118 ± 0.003
$14 < {p_{\mathrm{T}}}^{\mathrm{B}} < 40$	0.120 ± 0.002

(d) Results as a function of the B-meson pseudorapidity.

Range	$\mathcal{R}$
$2.0 < \eta^{\mathrm{B}} < 2.5$	0.127 ± 0.004
$2.5 < \eta^{\mathrm{B}} < 2.8$	0.131 ± 0.003
$2.8 < \eta^{\mathrm{B}} < 3.0$	0.129 ± 0.003
$3.0 < \eta^{\mathrm{B}} < 3.2$	0.130 ± 0.002
$3.2 < \eta^{\mathrm{B}} < 3.4$	0.126 ± 0.002
$3.4 < \eta^{\mathrm{B}} < 3.6$	0.125 ± 0.002
$3.6 < \eta^{\mathrm{B}} < 3.8$	0.127 ± 0.002
$3.8 < \eta^{\mathrm{B}} < 4.0$	0.128 ± 0.003
$4.0 < \eta^{\mathrm{B}} < 4.3$	0.129 ± 0.003
$4.3 < \eta^{\mathrm{B}} < 6.4$	0.130 ± 0.002

(e) Results as a function of the B-meson rapidity.

Range	$\mathcal{R}$
$2.0 < y^{\mathrm{B}} < 2.5$	0.130 ± 0.003
$2.5 < y^{\mathrm{B}} < 3.0$	0.127 ± 0.002
$3.0 < y^{\mathrm{B}} < 3.5$	0.126 ± 0.002
$3.5 < y^{\mathrm{B}} < 4.0$	0.128 ± 0.003
$4.0 < y^{\mathrm{B}} < 4.5$	0.127 ± 0.005

A.6 Plotted efficiency-corrected yield ratios as a function of Δy

Given the availability of data at different center-of-mass energies, results can be compared as a function of the variable

$$\Delta y = y_{\rm beam} - y^B$$

where $y_{\rm beam}$ is the rapidity of the incoming proton beam and $y^{\rm B}$ the B-meson rapidity. This variable is typically defined in association with the transport of the baryon number from the initial to the final state in $pp \to NX$ reactions, where N is a generic baryon and X can be any accompanying process. However, it can be useful also to understand the hadronization process for mesons.

The results of the efficiency-corrected yield ratios as a function of Δy are shown in Fig. 7 as obtained by shifting those as a function of $y^{\rm B}$ by the corresponding $y_{\rm beam}$. This variable is useful for comparison with ATLAS and CMS experiments. As an example, LHCb data at $\sqrt{s} = 13\,\text{TeV}/c$ (or $y_{\rm beam} = 10.2$) and rapidity $y \simeq 2$ could be compared with ATLAS/CMS data at $\sqrt{s} = 7\,\text{TeV}/c$ ($y_{\rm beam} = 9.6$) and rapidity $y \simeq 1$; a region otherwise unavailable to LHCb at $\sqrt{s} = 7\,\text{TeV}/c$.

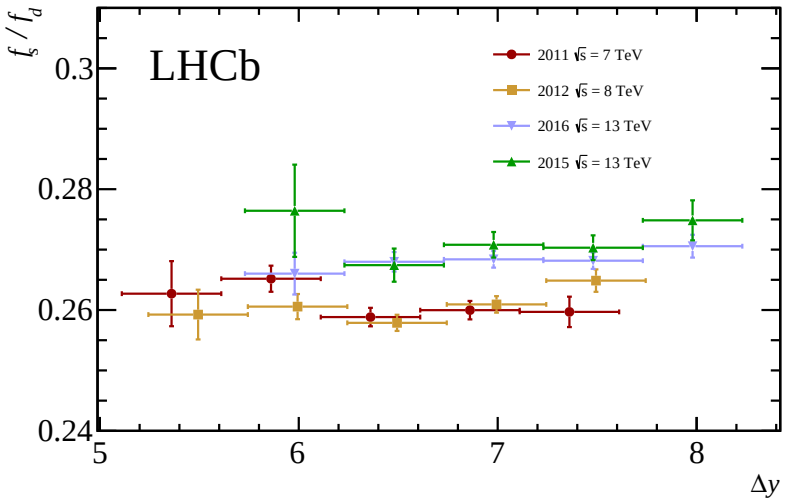

Figure 7: Efficiency-corrected $B_s^0 \to {\rm J}/\psi\,\phi$ and $B^+ \to {\rm J}/\psi\,K^+$ yield ratios ($\mathcal{R}$) in bins of Δy for different samples. The ratios are scaled to match the measured f_s/f_d value.

A.7 Numerical and plotted ratios in bins of $p_{\mathrm{T}}^{\mathrm{B}}$ for different pp collision energies

Table 3: Efficiency-corrected $B_s^0 \to \mathrm{J}/\psi\,\phi$ and $B^+ \to \mathrm{J}/\psi\,K^+$ yield ratios in bins of B-meson transverse momentum $p_{\mathrm{T}}^{\mathrm{B}}$, separately for the three pp collision energies.

(a) Results at $\sqrt{s} = 7$ TeV/c

Range [GeV/c]	$\mathcal{R}$
$0.5 < p_{\mathrm{T}}^{\mathrm{B}} < 2$	0.119 ± 0.003
$2 < p_{\mathrm{T}}^{\mathrm{B}} < 3$	0.127 ± 0.003
$3 < p_{\mathrm{T}}^{\mathrm{B}} < 4$	0.120 ± 0.002
$4 < p_{\mathrm{T}}^{\mathrm{B}} < 5$	0.122 ± 0.002
$5 < p_{\mathrm{T}}^{\mathrm{B}} < 6$	0.122 ± 0.002
$6 < p_{\mathrm{T}}^{\mathrm{B}} < 7$	0.128 ± 0.003
$7 < p_{\mathrm{T}}^{\mathrm{B}} < 8$	0.129 ± 0.003
$8 < p_{\mathrm{T}}^{\mathrm{B}} < 9$	0.129 ± 0.003
$9 < p_{\mathrm{T}}^{\mathrm{B}} < 10$	0.115 ± 0.003
$10 < p_{\mathrm{T}}^{\mathrm{B}} < 12$	0.116 ± 0.003
$11 < p_{\mathrm{T}}^{\mathrm{B}} < 14$	0.118 ± 0.003
$14 < p_{\mathrm{T}}^{\mathrm{B}} < 40$	0.117 ± 0.003

(b) Results at $\sqrt{s} = 8$ TeV/c

Range [GeV/c]	$\mathcal{R}$
$0.5 < p_{\mathrm{T}}^{\mathrm{B}} < 2$	0.121 ± 0.002
$2 < p_{\mathrm{T}}^{\mathrm{B}} < 3$	0.121 ± 0.002
$3 < p_{\mathrm{T}}^{\mathrm{B}} < 4$	0.120 ± 0.002
$4 < p_{\mathrm{T}}^{\mathrm{B}} < 5$	0.127 ± 0.002
$5 < p_{\mathrm{T}}^{\mathrm{B}} < 6$	0.125 ± 0.002
$6 < p_{\mathrm{T}}^{\mathrm{B}} < 7$	0.125 ± 0.002
$7 < p_{\mathrm{T}}^{\mathrm{B}} < 8$	0.121 ± 0.002
$8 < p_{\mathrm{T}}^{\mathrm{B}} < 9$	0.122 ± 0.002
$9 < p_{\mathrm{T}}^{\mathrm{B}} < 10$	0.125 ± 0.002
$10 < p_{\mathrm{T}}^{\mathrm{B}} < 12$	0.125 ± 0.002
$11 < p_{\mathrm{T}}^{\mathrm{B}} < 14$	0.119 ± 0.002
$14 < p_{\mathrm{T}}^{\mathrm{B}} < 40$	0.119 ± 0.002

(c) Results at $\sqrt{s} = 13$ TeV/c.

Range [GeV/c]	$\mathcal{R}$
$0.5 < p_{\mathrm{T}}^{\mathrm{B}} < 2$	0.133 ± 0.002
$2 < p_{\mathrm{T}}^{\mathrm{B}} < 3$	0.132 ± 0.002
$3 < p_{\mathrm{T}}^{\mathrm{B}} < 4$	0.134 ± 0.002
$4 < p_{\mathrm{T}}^{\mathrm{B}} < 5$	0.132 ± 0.002
$5 < p_{\mathrm{T}}^{\mathrm{B}} < 6$	0.134 ± 0.002
$6 < p_{\mathrm{T}}^{\mathrm{B}} < 7$	0.129 ± 0.002
$7 < p_{\mathrm{T}}^{\mathrm{B}} < 8$	0.131 ± 0.002
$8 < p_{\mathrm{T}}^{\mathrm{B}} < 9$	0.129 ± 0.002
$9 < p_{\mathrm{T}}^{\mathrm{B}} < 10$	0.128 ± 0.002
$10 < p_{\mathrm{T}}^{\mathrm{B}} < 12$	0.128 ± 0.002
$11 < p_{\mathrm{T}}^{\mathrm{B}} < 14$	0.118 ± 0.002
$14 < p_{\mathrm{T}}^{\mathrm{B}} < 40$	0.121 ± 0.002

The statistical significance of the f_s/f_u dependence on $p_{\mathrm{T}}^{\mathrm{B}}$ at each pp collision energy is estimated by fitting the efficiency-corrected $B_s^0 \to \mathrm{J}/\psi\,\phi$ and $B^+ \to \mathrm{J}/\psi\,K^+$ yield ratios ($\mathcal{R}$, see Table 3b and Fig. 3b of the main text) distributions with a function $A_{p_{\mathrm{T}}^{\mathrm{B}}} \cdot \exp(k_{p_{\mathrm{T}}^{\mathrm{B}}} \cdot p_{\mathrm{T}}^{\mathrm{B}})$ under two hypotheses: one where no variation is allowed and the slope parameter, $k_{p_{\mathrm{T}}^{\mathrm{B}}}$, is fixed to zero and one with $k_{p_{\mathrm{T}}^{\mathrm{B}}}$ left free. The χ^2 difference between the two cases is used as a test statistic and its p-value is determined from the χ^2 distribution with one degree of freedom. The results are $k_{p_{\mathrm{T}}^{\mathrm{B}}} = -(1.24 \pm 0.73) \times 10^{-3}\,\mathrm{GeV}^{-1}c$ ($2.1\,\sigma$), $k_{p_{\mathrm{T}}^{\mathrm{B}}} = -(0.59 \pm 0.39) \times 10^{-3}\,\mathrm{GeV}^{-1}c$ ($1.5\,\sigma$) and $k_{p_{\mathrm{T}}^{\mathrm{B}}} = -(4.40 \pm 0.67) \times 10^{-3}\,\mathrm{GeV}^{-1}c$ ($8.7\,\sigma$) for 7 TeV/c, 8 TeV/c and 13 TeV/c samples, respectively. The two-sided significances are given in the brackets.